

Pseudo-Quantum Criticality in Electron Liquids Exhibited in Expanded Alkali Metals

Hideaki Maebashi and Yasutami Takada

Institute for Solid State Physics, University of Tokyo, Kashiwa, Chiba 277-8581, Japan

(Dated: November 8, 2018)

With paying special attention to the divergence in the compressibility κ , we study the Coulombic screening in alkali metals to find singular long-range fluctuations in the electronic polarization originating from this divergence. As a consequence of this singularity, we predict the decrease of the equilibration distance between ions against the increase of r_s the Wigner-Seitz radius of valence electrons, provided that the condition of $2r_c < r_s < 4r_c$ is satisfied with r_c the ion-core radius. This prediction is in good quantitative agreement with the recent experiment on liquid Rb.

PACS numbers: 71.10.Ca, 71.45.Gm, 61.25.Mv, 05.70.Jk

According to the recent high-resolution measurement of x-ray diffraction for expanded liquid Rb [1], an average distance between nearest-neighbor ions R_{NN} , as determined by the first-peak position in the radial distribution function $g(R)$, *decreases* with increasing R_0 the Wigner-Seitz (WS) radius of ions. This is in sharp contrast with the normal situation in compressed liquid alkali metals in which R_{NN} increases with R_0 [2, 3, 4, 5]. In solid Rb the valence-electron density n is specified by $r_s = 5.2$ with r_s being the WS radius of electrons (in atomic units which we take throughout this Letter), very close to $r_s = 5.25$ at which the compressibility κ of the 3D electron gas diverges [6]. Thus n in expanded liquid Rb is in the range of $r_s > 5.25$ where κ is negative [7]. In this Letter, we shall explain this unexpected contraction of R_{NN} by focusing on the divergence, rather than the negativeness, of κ as a key issue.

At arbitrary n , the compressibility sum rule relates κ to the polarization function $\Pi^R(q, \omega)$ (with the superscript R denoting the retarded form) through $\lim_{q \rightarrow 0} \Pi^R(q, 0) = n^2 \kappa$. Hence, near the critical density of $r_s = 5.25$, $\Pi^R(q, \omega)$ becomes singular in the limits of $q/p_F \rightarrow 0$ and $\omega/v_F q \rightarrow 0$ with p_F and v_F being, respectively, the Fermi wave number and the free-electron Fermi velocity. More specifically, we find that $\Pi^R(q, \omega)$ is well characterized by such a singular form as

$$\Pi^R(q, \omega) \simeq n^2 \kappa_F \xi_F^{-2} / (\xi^{-2} + q^2 - i\omega/\Gamma q), \quad (1)$$

where $\xi^2 = (\kappa/\kappa_F)\xi_F^2$, $\Gamma = (2/\pi)v_F\xi_F^2$, and $\xi_F^{-2} = 12p_F^2$ with κ_F the free-electron compressibility. Note that near the quantum critical point (QCP) of dynamical exponent 3 [8], the response function takes exactly the same form as in Eq. (1). In the electron gas, however, there is no true phase transition (and in fact “the correlation length” ξ turns into a pure imaginary value for negative κ), owing to the fact that $\Pi^R(q, \omega)$ in this case represents response to a total of external and induced charges, making it acausal [9]. One of the interesting consequences of Eq. (1) near this “pseudo-quantum critical point” is the softening of excitonic collective modes, as featured by the dispersion relation of $\omega = (2/\pi)|\kappa_F/\kappa + q^2\xi_F^2|v_F q$ [10].

The classical or Coulombic screening of ions near this pseudo-QCP poses a distinct problem from the quantum or Kondo screening near the true QCP [11] and

deserves special attention, basically because it is useful in clarifying the important physics of the coupling between the $q = 0$ singularity in the Coulomb interaction, $v(q) = 4\pi/q^2$, and the singular fluctuations in $\Pi^R(q, 0)$. Another important aspect of the problem is the fact that the ions in alkali metals are not point charges but complexes of a nucleus and core electrons surrounding it, the feature of which can be well captured by a suitable pseudopotential $V_{\text{ps}}(q)$. This complex structure combined with the pseudo-QCP makes the observable phenomena intriguing, in which an important role is played by the presence of a characteristic wave number q_0 (proportional to the inverse of the core-electron radius r_c) at which $V_{\text{ps}}(q)$ vanishes due to the orthogonality between valence- and core-electron wave functions [12].

In this Letter, we report on our finding that the pseudo-quantum criticality is intimately connected with the appearance of a local minimum in the electrostatic potential $\phi(q)$ at $q = 0$ for some range of r_s (see Fig. 1). This minimum is shown to be brought about by (i) the Thomas-Fermi-type screening with the singular polarization and (ii) the subsequent rearrangement of the charge distribution in response to the resulting screening hole. The first process induces the contraction of the equilibration distance between ions, while the second acts in the opposite way. In expanded alkali metals, this second process is suppressed by the presence of q_0 in $V_{\text{ps}}(q)$, leading to the experimental results [1] with which our theoretical results of $g(R)$ obtained by systematic Monte-Carlo simulations for Rb ions are in good accord.

In terms of $\Pi^R(q, 0)$, we can write $\phi(q)$ induced by a point charge in the 3D electron gas as

$$\phi(q) = v(q)/[1 + v(q)\Pi^R(q, 0)]. \quad (2)$$

Using the exchange-correlation kernel $f_{\text{xc}}(q, \omega)$, we can give a formally exact expression for $\Pi^R(q, \omega)$ as $\Pi^R(q, \omega) = [\Pi^{0R}(q, \omega)^{-1} + f_{\text{xc}}(q, \omega)]^{-1}$, where $\Pi^{0R}(q, \omega)$ is the free-electron polarization function. Since an accurate parameterization of the diffusion Monte Carlo (DMC) data for $f_{\text{xc}}(q, 0)$ is available [13], the virtually exact $\phi(q)$ is known. (See the solid curves in Fig. 1(a).) The DMC data reveal that $f_{\text{xc}}(q, 0)$ is flat near $q = 0$, e.g., $f_{\text{xc}}(q, 0) - \lim_{q \rightarrow 0} f_{\text{xc}}(q, 0) \sim O(q^{16})$ for $r_s = 5$ [13], allowing us to derive the result in Eq. (1) for $q/p_F \ll 1$

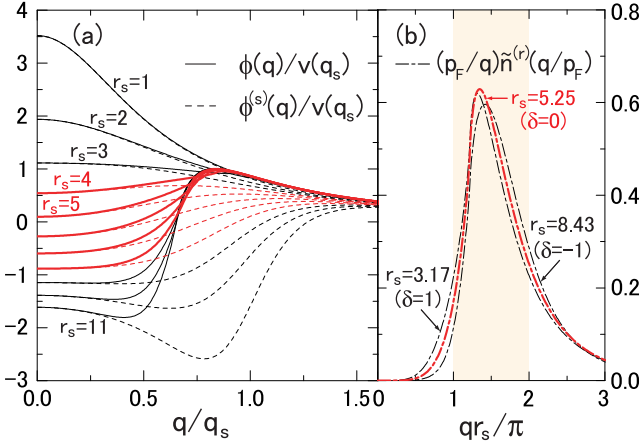


FIG. 1: (a) Electrostatic potential $\phi(q)$ scaled by $v(q_s)$ with $q_s = \sqrt{q_{\text{TF}}/\xi_{\text{F}}}$ as a function of q/q_s with changing r_s from 1 to 11 by 1 (the solid curves from top to bottom), together with the corresponding screening potential $\phi^{(s)}(q)$ in Eq. (4) by the broken curves. (b) Rearrangement of the charge distribution due to the screening hole $\tilde{n}^{(r)}(q/p_{\text{F}})$ divided by q/p_{F} , which is properly scaled in Eq. (6), as a function of qr_s/π . The “distance” from the pseudo-QCP is defined as $\delta = \phi(0)/v(q_s)$.

and $\omega/v_{\text{F}}q \ll 1$ under the assumption that the limits of $q \rightarrow 0$ and $\omega \rightarrow 0$ are interchangeable for $f_{\text{xc}}(q, \omega)$.

Although $\Pi^{0R}(q, 0)$ itself is specified only by $p_{\text{F}}^{-1} = \alpha r_s$ with $\alpha = (4/9\pi)^{1/3}$, a unique length scale for this function, consideration of the coupling to the Coulomb interaction evokes another length scale, $q_{\text{TF}}^{-1} = (\pi\alpha r_s/4)^{1/2}$, as characterized by $v(q)\Pi^{0R}(q, 0) \simeq q_{\text{TF}}^2/q^2$ for $q \rightarrow 0$. For the full polarization function $\Pi^R(q, 0)$, Eq. (1) indicates $|\xi|$ as a characteristic length scale which becomes much longer than $\xi_{\text{F}} \approx p_{\text{F}}^{-1}$ for $\kappa/\kappa_{\text{F}} \gg 1$. Eventually at the pseudo-QCP, concomitantly with the divergence of $|\xi|$, a new length scale, $q_s^{-1} = \sqrt{\xi_{\text{F}}/q_{\text{TF}}}$, emerges for the coupling to the Coulomb interaction, as characterized by $v(q)\Pi^R(q, 0) \simeq q_s^4/q^4$ for $q \rightarrow 0$.

Keeping those length scales in mind, we represent $\phi(q)$ in an expansion form around $q = 0$ for arbitrary n as

$$\phi(q) = v(q_s)[\delta + (1 - \delta^2)(q/q_s)^2 + O(q^4)]. \quad (3)$$

Here we have introduced $\delta [\equiv (\kappa_{\text{F}}/\kappa)/(q_{\text{TF}}\xi_{\text{F}})]$ as a key quantity describing the “distance” from the pseudo-QCP. In Eq. (3), the coefficient of the q^2 term is positive for $|\delta| < 1$ corresponding to $3.17 < r_s < 8.43$, which clarifies the reason why $\phi(q)$ in Fig. 1(a) exhibits a local minimum at $q = 0$ only in this range of r_s . We shall call this range the pseudo-quantum critical region, in which alkali metals, Na, K, Rb, and Cs, are included.

In order to obtain a deeper insight into the Coulombic screening in the presence of the singular contribution in $\Pi^R(q, 0)$, let us write $\phi(q)$ as

$$\phi(q) = v(q)[1 - n_{\text{ind}}(q)] = \phi^{(s)}(q) + \phi^{(r)}(q), \quad (4)$$

where $n_{\text{ind}}(q) [\equiv v(q)\Pi^R(q, 0)/(1 + v(q)\Pi^R(q, 0))]$ is the electron density distribution induced by the point charge

and $\phi^{(s)}(q)$ is defined by substituting the singular polarization, Eq. (1), into Eq. (2) as $\phi^{(s)}(q) = v(q)[1 - n_{\text{ind}}^{(s)}(q)]$ with $n_{\text{ind}}^{(s)}(q)$, given by

$$n_{\text{ind}}^{(s)}(q) = [1 + \delta(q/q_s)^2 + (q/q_s)^4]^{-1}. \quad (5)$$

It is easily verified that when $r_s \rightarrow 0$, Eq. (5) is reduced to the standard Thomas-Fermi screening charge, $n_{\text{ind}}^{(s)}(q) \rightarrow q_{\text{TF}}^2/(q_{\text{TF}}^2 + q^2)$. Thus we may regard $\phi^{(s)}(q)$ as the Thomas-Fermi-type screening potential with the singular polarization. In Fig. 1(a), $\phi^{(s)}(q)$ is plotted by the broken curves with changing r_s from 1 to 11 by 1.

The residual term in Eq. (4), $\phi^{(r)}(q)$, is the electrostatic potential due to the rearrangement of the induced charge from $n_{\text{ind}}^{(s)}(q)$ to $n_{\text{ind}}(q)$, amounting to $\phi^{(r)}(q) = v(q)n^{(r)}(q)$ with $n^{(r)}(q) \equiv n_{\text{ind}}^{(s)}(q) - n_{\text{ind}}(q)$. Since the singular long-range part $n_{\text{ind}}^{(s)}(q)$ is extracted from $n_{\text{ind}}(q)$, we speculate that $n^{(r)}(q)$ is characterized only by the length scale p_{F}^{-1} , implying that $n^{(r)}(q)$ should be expressed in terms of some universal function of q/p_{F} . This speculation is checked by casting $n^{(r)}(q)$ into the form as

$$n^{(r)}(q) = (2 + \delta)^{-1}(q_{\text{TF}}/q_s)^2 \tilde{n}^{(r)}(q/p_{\text{F}}). \quad (6)$$

Here we have determined the prefactor by respecting the result of $n_{\text{ind}}^{(s)}(q_s) = (2 + \delta)^{-1}$. In Fig. 1(b), we plot the obtained $\tilde{n}^{(r)}(x)/x$ with $x = q/p_{\text{F}}$ for $\delta = 0$ and ± 1 , from which we see that $\tilde{n}^{(r)}(x)/x$, having a peak structure for $\pi/r_s < q < 2\pi/r_s$, may well be regarded as universal in the entire pseudo-quantum critical region.

In calculating $\tilde{V}_{\text{ii}}(R)$ the effective interaction between ions, we resort to second-order perturbation with respect to $V_{\text{ps}}(q)$ [14]. For R outside the core region, we obtain

$$\tilde{V}_{\text{ii}}(R) = \frac{1}{2\pi^2 R} \int_0^\infty \rho_{\text{ps}}(q)^2 \phi(q) q \sin(qR) dq, \quad (7)$$

where $\rho_{\text{ps}}(q)$ is the effective charge of the ion, given by $\rho_{\text{ps}}(q) = (q^2/4\pi)V_{\text{ps}}(q)$. In general, the charge neutrality of the whole system imposes $\rho_{\text{ps}}(0) = 1$. For $r_c > 0$, $\rho_{\text{ps}}(q)$ vanishes at $q = q_0$. In the limit of $r_c \rightarrow 0$ (or $q_0 \rightarrow \infty$), however, $\rho_{\text{ps}}(q) = 1$ for arbitrary q , which reduces $\tilde{V}_{\text{ii}}(R)$ into $\phi(R)$, the inverse Fourier transform of $\phi(q)$. In the following specific calculations, for simplicity, we employ the Ashcroft empty-core pseudopotential, for which $\rho_{\text{ps}}(q) = \cos qr_c$, but our conclusions do not depend on the detailed shape of $V_{\text{ps}}(q)$ very much.

In accordance with Eq. (4), we shall divide $\tilde{V}_{\text{ii}}(R)$ in Eq. (7) into two components as

$$\tilde{V}_{\text{ii}}(R) = \tilde{V}_{\text{ii}}^{(s)}(R) + \tilde{V}_{\text{ii}}^{(r)}(R), \quad (8)$$

where $\tilde{V}_{\text{ii}}^{(s)}(R)$ and $\tilde{V}_{\text{ii}}^{(r)}(R)$ are, respectively, defined by using $\phi^{(s)}(q)$ and $\phi^{(r)}(q)$ instead of $\phi(q)$ in Eq. (7). Since $n_{\text{ind}}^{(s)}(q)$ is given in a simple analytic function, we can analyze $\tilde{V}_{\text{ii}}^{(s)}(R)$ by pursuing the poles of $\phi^{(s)}(q)$ or equivalently those of $n_{\text{ind}}^{(s)}(q)$ in the complex q space. According

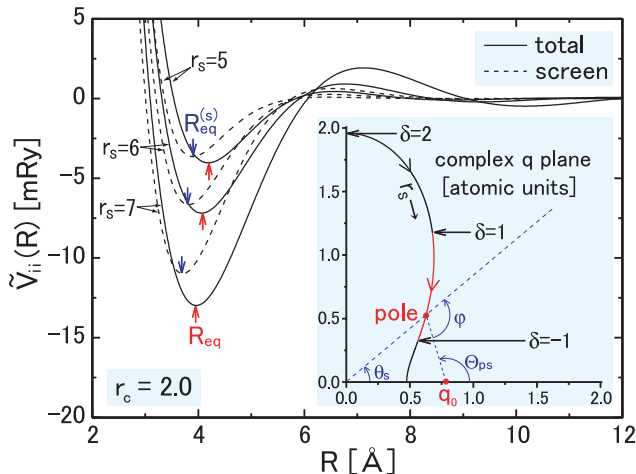


FIG. 2: Effective interaction between ions, $\tilde{V}_{ii}(R)$, with using the empty-core pseudopotential with $r_c = 2.0$, for $r_s = 5, 6$, and 7 (the solid curves). The broken curves represent $\tilde{V}_{ii}^{(s)}(R)$ in Eq. (9). The inset shows the trajectory of the screening pole $q_s e^{i\theta_s}$ with increasing r_s in the complex q plane.

to Eq. (5), all the poles are on the imaginary axis for $\delta > 2$, while they deviate from the axis for $\delta < 2$ (see the inset of Fig. 2), implying that the “screening length” in the Thomas-Fermi-type screening potential changes into a complex number, so that the resulting potential shows a damped oscillatory behavior. As δ decreases, the oscillation amplitude increases and eventually for $\delta < 1$, the short-range attractive part develops in $\tilde{V}_{ii}^{(s)}(R)$. Note that this oscillation related to the pseudo-quantum criticality is distinct from the Friedel oscillation, because the latter does not originate from those poles but the branch-cut singularity in $\phi(q)$.

For $|\delta| < 2$, the poles in the upper-half complex q plane reside at $q_s e^{i\theta_s}$ and $-q_s e^{-i\theta_s}$ with $\theta_s = (1/2) \cos^{-1}(-\delta/2)$. Writing $\rho_{ps}(q_s e^{i\theta_s})$ as $Z_{ps} e^{i\Theta_{ps}}$, we obtain $\tilde{V}_{ii}^{(s)}(R)$ as

$$\tilde{V}_{ii}^{(s)}(R) = Z_{ps}^2 \frac{\sin(2\varphi - q_s R \cos \theta_s)}{R \sin 2\theta_s} e^{-q_s R \sin \theta_s}, \quad (9)$$

with $\varphi = \theta_s - \Theta_{ps} + \pi$. This analytic result with $r_c = 2.0$ is plotted in Fig. 2 by the broken curves for $r_s = 5, 6$, and 7 , in comparison with the corresponding numerical result for $\tilde{V}_{ii}(R)$ (the solid curves). The global minimum in $\tilde{V}_{ii}(R)$ determines the equilibration distance between ions, R_{eq} , which is found to decrease with increasing r_s . The same is true for $R_{eq}^{(s)}$ the equilibration distance determined through $\tilde{V}_{ii}^{(s)}(R)$, suggesting that the main feature of R_{eq} will be studied by examining $R_{eq}^{(s)}$. An approximate result for $R_{eq}^{(s)}$ is obtained from Eq. (9) as

$$R_{eq}^{(s)} \approx (2\varphi + \pi/2)/(q_s \cos \theta_s) = (4\varphi + \pi)/q_s \sqrt{2 - \delta}. \quad (10)$$

A rather extensive examination of various factors in Eq. (9) reveals that $R_{eq}^{(s)}$ is mainly controlled by φ . As shown in the inset of Fig. 2, the phase θ_s decreases as the

pole $q_s e^{i\theta_s}$ evolves along the trajectory with increasing r_s . On the other hand, the phase Θ_{ps} increases, because it is approximately given by the phase of $q - q_0$ itself, as can be seen by expanding $\rho_{ps}(q)$ around $q = q_0$. Therefore, in a combined manner, both changes contribute to the decrease of the phase φ , leading eventually to the contraction of $R_{eq}^{(s)}$ with the increase of r_s . Incidentally, for very large q_0 as in the case of a point charge, Θ_{ps} hardly changes. Thus in such a case, only the phase θ_s contributes to the decrease of $R_{eq}^{(s)}$.

The presence of $\tilde{V}_{ii}^{(r)}(R)$ in Eq. (8) manifests itself in the difference between R_{eq} and $R_{eq}^{(s)}$. This residual interaction is determined by $n^{(r)}(q)$ in Eq. (6). Since it is scaled by p_F^{-1} , the resulting interaction is necessarily scaled by the same length scale or αr_s , indicating that $\tilde{V}_{ii}^{(r)}(R)$ contributes to increasing $R_{eq}^{(s)}$ with r_s . In this context, it is important to note that $n^{(r)}(q)$ has a sharp peak structure as shown in Fig. 1 (b). Thus, if $\rho_{ps}(q)$ is small in the peak region of $n^{(r)}(q)$ as realized by the condition of $\pi/r_s < q_0 < 2\pi/r_s$, the contribution of $\tilde{V}_{ii}^{(r)}(R)$ is strongly suppressed, making R_{eq} approach $R_{eq}^{(s)}$. This suppression never occurs in the point-charge case.

In Fig. 3, we show the overall behavior of R_{eq} with the change of $r_s/2r_c$, which is obtained numerically with using the empty-core pseudopotential. The broken lines correspond to $\delta = 1$ ($r_s = 3.17$), $\delta = 0$ ($r_s = 5.25$), and $\delta = -1$ ($r_s = 8.43$), showing the pseudo-quantum critical region. The contraction of R_{eq} is clearly seen for $2r_c < r_s < 4r_c$ in accordance with $\pi/r_s < q_0 < 2\pi/r_s$, where $q_0 = \pi/2r_c$. Although the global minimum of $\tilde{V}_{ii}(R)$ is obtained at its first minimum for $\delta < 1$, the second minimum becomes lower than the first one for $\delta > 1$, making R_{eq} jump, which is not shown in Fig. 3. For $\delta < -1$, the situation is completely different because of the shift of the global minimum of $\phi(q)$ to a finite q (see

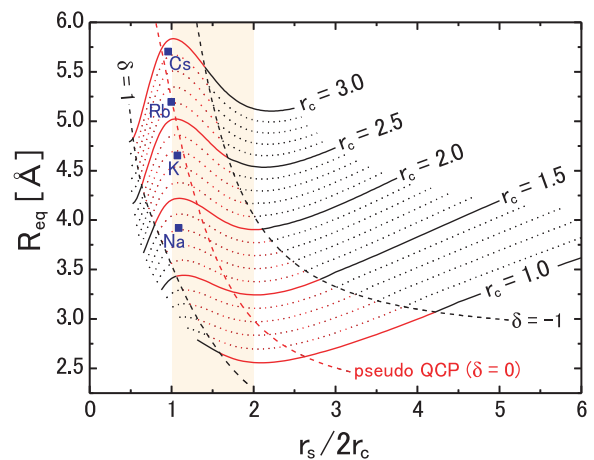


FIG. 3: Equilibration distance between ions, R_{eq} , for the empty-core pseudopotential with changing r_c from 1.0 to 3.0 by 0.1 versus the ratio of the WS radius of the electrons r_s to the core diameter $2r_c$.

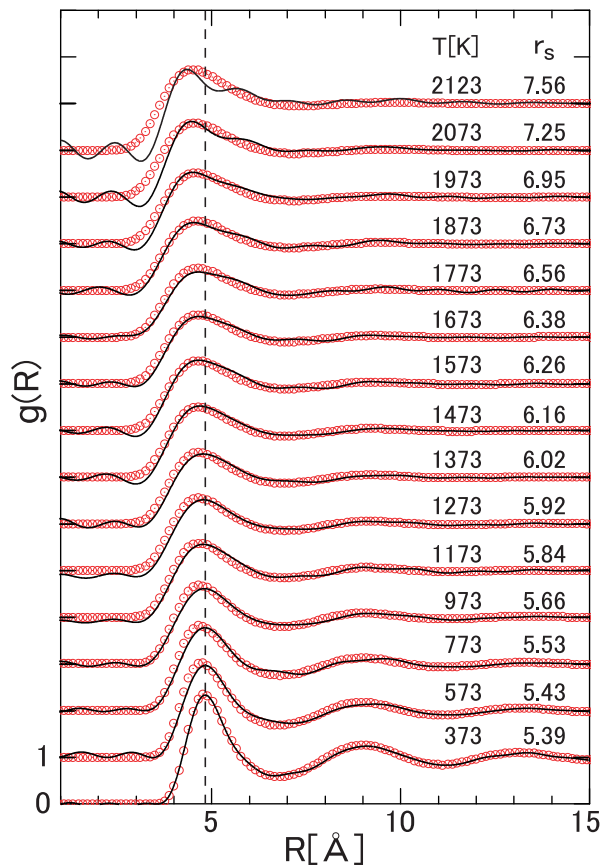


FIG. 4: Comparison between our theoretical results of $g(R)$ obtained by the canonical Monte-Carlo simulations (the open circles) and the experimental results in Ref. [1] (the solid curves). The broken line denotes R_{NN} of $g(R)$ at 373 K.

Fig. 1). This may be related to the instability toward the Wigner transition.

The contraction of R_{eq} may be explained from a geometrical point of view. Inserting two ions into the electron liquid excludes the valence electrons from the core regions owing to the orthogonality between valence- and core-electron wave functions. For the case of $2r_c < r_s <$

$4r_c$, the rearrangement of the induced charge distribution due to the screening hole is restricted, because the WS radius r_s , which is the typical length of the electron liquid, is comparable with the diameter of the excluded volume. Then, $\tilde{V}_{ii}(R)$ is dominated by the complex screening $\tilde{V}_{ii}^{(s)}(R)$ in the pseudo-quantum critical region. On the other hand, when $r_s > 4r_c$, the valence electrons recognize the ion core virtually as a point charge, so that the problem is reduced to R_{eq} between two point charges which is an increasing function of r_s . In Fig. 3, we have also plotted R_{eq} for solid alkali metals, Na, K, Rb, and Cs. Since $r_s/2r_c \simeq 1$ in these metals, the contraction of R_{eq} is generally expected in the expanded alkali metals.

Finally, in Fig. 4, we present the canonical Monte-Carlo results of the radial distribution function $g(R)$ for 500 classical particles interacting with each other through $\tilde{V}_{ii}(R)$ in Eq. (7) at finite temperatures, together with the experimental results in Ref. [1]. For liquid Rb, we have used the empty-core pseudopotential with $r_c = 2.4$ [15]. The agreement between theory and experiment is good not only for the first-peak position but also for the overall change of $g(R)$ with increasing r_s and temperature.

In summary, we have shown that the pseudo-quantum criticality in electron liquids transforms the standard Thomas-Fermi screening into the complex screening characterized by the development of a short-range attractive part in the screened Coulomb interaction. For $2r_c < r_s < 4r_c$, the core-valence orthogonality promotes this complex-screening effect by suppressing the rearrangement of the induced charge due to the screening hole, leading to the contraction of the equilibration distance between ions with increasing r_s in good agreement with experiment on expanded liquid Rb.

The authors acknowledge K. Matsuda and K. Tamura for providing their experimental data. The authors also thank T. Kato, M. Shimomoto, and M. Shiroishi for helpful comments on the Monte-Carlo simulations. The computational work is done using the facilities of Supercomputer Center, ISSP, UT. This work is partially supported by a Grant-in-Aid for Scientific Research in Priority Areas (No.17064004) of MEXT, Japan.

[1] K. Matsuda *et al.*, Phys. Rev. Lett. **98**, 096401 (2007).
[2] For a recent review, see Y. Katayama and K. Tsuji, J. Phys. Condens. Matter **15**, 6085 (2003).
[3] S. Falconi *et al.*, Phys. Rev. Lett. **94**, 125507 (2005).
[4] E. Gregoryanz *et al.*, Phys. Rev. Lett. **94**, 185502 (2005).
[5] F. Shimojo *et al.*, Phys. Rev. B **55**, 5708 (1997); J. Phys. Soc. Jpn. **67**, 3471 (1998).
[6] D.M. Ceperley and B.J. Alder, Phys. Rev. Lett. **45**, 567 (1980); S.H. Vosko *et al.*, Can. J. Phys. **58**, 1200 (1980); Y. Takada, Phys. Rev. B **43**, 5979 (1991).
[7] It is noted that the valence-electron system is stable against phase separation even though $\kappa < 0$, because the total compressibility of electrons and ions is positive.
[8] See, for example, S. Sachdev, *Quantum Phase Transition*

(Cambridge University Press, New York, 1999).
[9] O.V. Dolgov *et al.*, Rev. Mod. Phys. **53**, 81 (1981).
[10] Y. Takada, Phys. Rev. Lett. **87**, 226402 (2001); Y. Takada and H. Yasuhara, *ibid.* **89**, 216402 (2002); Y. Takada, J. Supercond. **18**, 785 (2005).
[11] H. Maebashi *et al.*, Phys. Rev. Lett. **88**, 226403 (2002); *ibid.* **95**, 207207 (2005).
[12] For example, see W.A. Harrison, *Electric Structure and the Properties of Solids* (Dover, New York, 1989).
[13] S. Moroni *et al.*, Phys. Rev. Lett. **75**, 689 (1995).
[14] For a review, see N.W. Ashcroft and D. Stroud, Solid State Phys. **33**, 1 (1978).
[15] E. Chacón *et al.*, Phys. Rev. B **52**, 9330 (1995).